# Concept of Central Tracking in PEP-N Experiment

J. Va'vra
*SLAC, Stanford University*

The paper describes a proposal of the central tracking in the PEP-N experiment. It follows the presentation [a] given at the PEP-N workshop in March 2001 at SLAC.

## 1. INTRODUCTION

The difficulties with various choices of tracking concepts in the PEP-N dipole magnet can be summarized as follows:

- A classical wire chamber with wires parallel to beam pipe would have very asymmetrical drift as a function of cell azimuth.
- A classical wire chamber with wires parallel to magnetic filed would have rather "ugly" vertex coverage, and a large mass right in the vertex region caused by the wire supporting end plate.
- A classical TPC with the electric field aligned with the magnetic field would have very large distortions because E versus B angle was as much as 18° at radial distance of 50 cm in the initial design, and possibly large low energy background, which normally goes through the beam pipe, can follow the magnetic field into the TPC active volume.

We have decided to pursue the TPC concept hoping that the TPC distortions can be dealt with a choice of gas and sophisticated laser calibration system, and the large background can be dealt with the robustness of the TPC concept if one runs very low gas gain. Furthermore, it was believed that the non-uniformity of the magnetic field would be improved by modifications of pole shapes.

## 2. TPC DESIGN

### 2.1. Field Uniformity of the Dipole Magnet

At the time of the workshop there were three magnetic field maps available: DV02 (initial design), DV03 (the first improvement) and DV06b (the best by the time of the workshop). Figure 1 shows the successive improvements in the field uniformity. The improvement is characterized in terms of Br and angle $\alpha$ between the magnetic field and the vertical electric field direction. One can see that the $\alpha$ angle is almost 18° in the DV02 design, and less than 5° in the DV06b design.

### 2.2. Calculation of TPC Distortions

The old Langevin theory [1] used in many TPC design proposals is only an approximate method and it is quite outdated today if one wants to do critical calculations such as large distortions. It calculates the electron drift velocity using the following equation:

$$\vec{v} = \frac{\mu}{1+(\omega\tau)^2}\left[\vec{E} + \frac{\omega\tau}{B}[\vec{E}\times\vec{B}] + (\omega\tau)^2\frac{\vec{E}\cdot\vec{B}}{B^2}B\right] \quad (1)$$

Its main weakness is not only that it does not have a capability to predict $\omega\tau$, but, in fact, it turns out that there is no single $\omega\tau$, which would explain all three drift velocity components.

I will use instead the Bagboltz-Monte program [2] to calculate the drift velocity components $v_{x,y,z}$ (E,B) gas. This particular program is presently considered the most correct method to calculate this problem, if one is dealing with the reasonably conventional gases. Once one knows the drift velocity components as a function of $z$-vertical (aligned with the dipole's field), one can calculate the distortions in the detecting plane using the following numerical integration:

$$\begin{aligned} dx &= \int_{t_1}^{t_2} v_x\, dt = \sum_i \langle v_x\rangle_i \frac{(dz)_i}{\langle v_z\rangle} \\ dy &= \int_{t_1}^{t_2} v_y\, dt = \sum_i \langle v_y\rangle_i \frac{(dz)_i}{\langle v_z\rangle}. \end{aligned} \quad (2)$$

In the following, I calculate the worst case distortion at $r = 50$ cm for the total drift of 50 cm. Figure 2 shows an example of such calculation for $80\%\mathrm{He} + 20\%\mathrm{CO_2}$ gas, which is considered a slow gas. The maximum distortion is less than 1 cm for the nominal field map DV02. Table I shows a summary of all calculations. One can see that fast gases have distortions at a level of up to 5 cm, the distortions in the slow gases can be brought to a level of a few mm. The slow gases have clearly

[a] http://pep-n.pd.infn.it/workshop/vavra.pdf

a) DV02 field map (initial design):

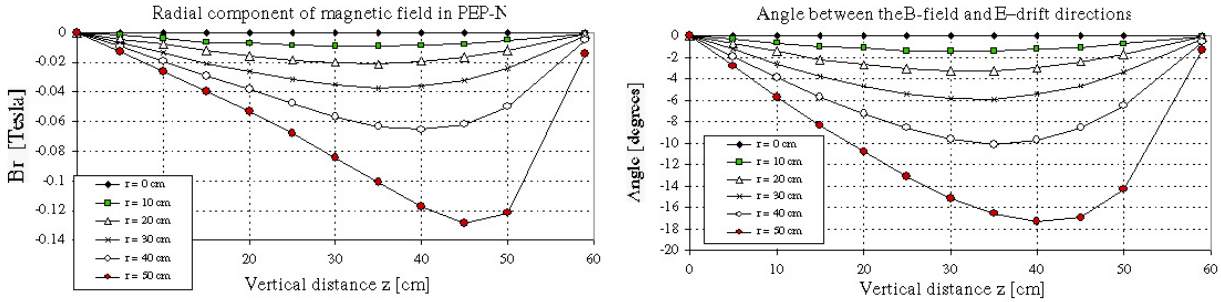


b) DV03 field map (iteration #1):

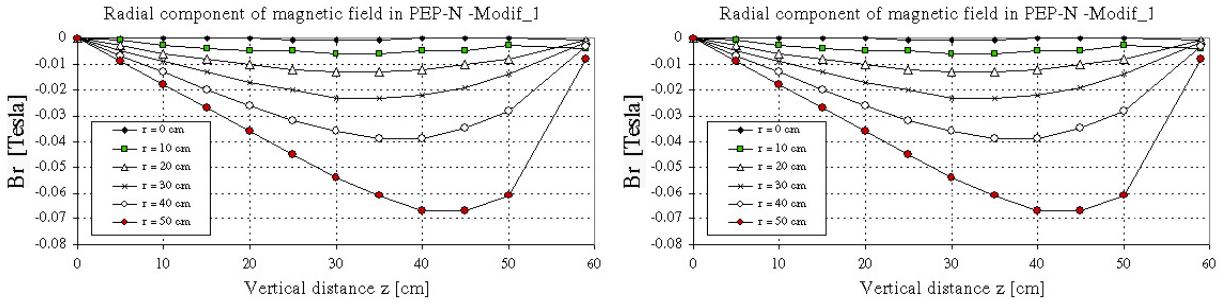


c) DV06b field map (the best design by the time of the workshop):

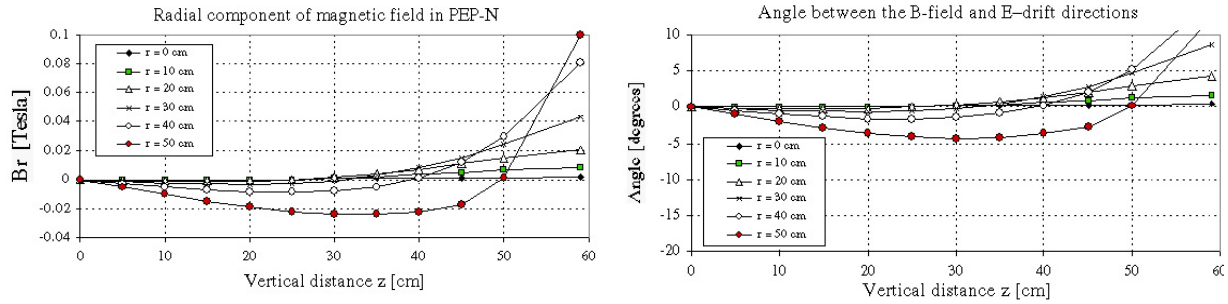


Figure 1: Prediction of magnetic field uniformity in the dipole magnet for three proposed solutions.

smaller distortions, however, one can utilize their advantage only if the background is sufficiently low to allow the total drift times up to 50$\mu$s, and the field cage has small distortions. Otherwise, one should use the fast gas. Table 1 shows that for the improved field map DV06, the ALEPH fast gas gives $\sim$ 1 cm of distortion.

Table II compares the PEP-N TPC distortions with other typical TPC designs. The table also shows the final reduction factor either already achieved to reach the final resolution. The NA-45 experiment proves that with a very good laser calibration system and with a lot of software effort one can achieve great improvements in the drift distortions [3]. To be able to reach the planned resolution in PEP-N TPC, the experiment needs to invest into (a) a good laser calibration system, (b) good external tracking, (c) keeping electrostatic distortions to minimum, and (d) keeping the systematic misalignments to minimum.

One should say that the similar dipole geometry has been tried in the past at LBL [4].

### 2.3. Expected Resolution Per Single Point

Following Bloom and Ronaldi [5], one arrives to the following expression for the single resolution point in the TPC with a typical wire & pad design:

$$\sigma^2_{\rm resol} \approx \frac{1}{N(h,w,b,\sigma_{\rm single})}\frac{\sigma^2_{\rm single}}{\cos^2\alpha} + \frac{b^2(\tan\Theta-\tan\Psi)^2\cos^2(\Theta-\alpha)}{12N_{\rm eff}(h,w,b,\sigma_{\rm single})} \qquad (3)$$

where

$\sigma_{\rm single}$ - single electron transverse diffusion,

$h$ - pad length,

$w$ - pad width,

$b$ - wire pitch,

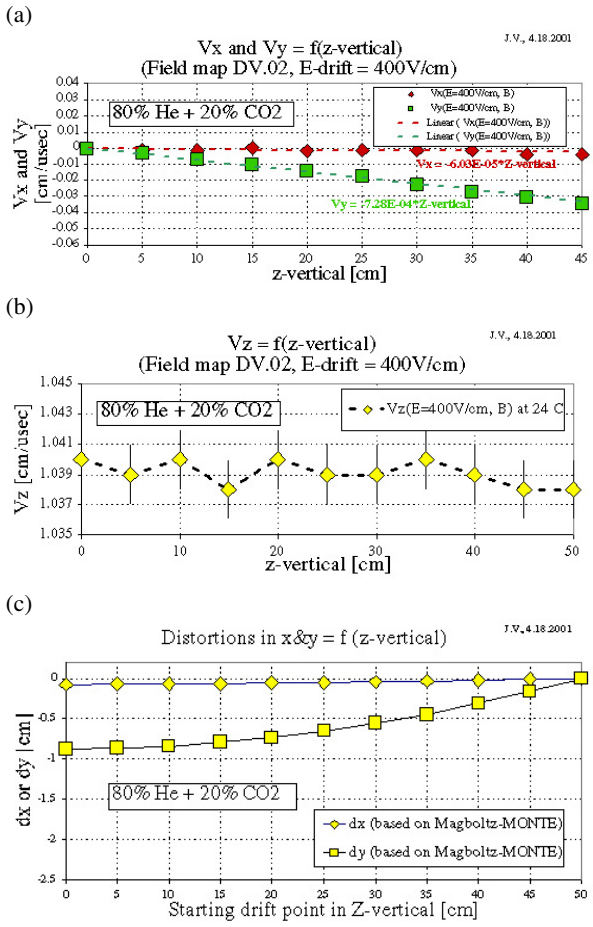


Figure 2: Calculation of the drift velocity components using the Bagboltz-MONTE program (a,b) and result of the subsequent numerical calculation of distortions in the detecting plane for a drift of 50 cm at radial distance of 50 cm, and for the magnetic field map DV02.

$N(h)$ - effective number of electrons per sample,

$N_{eff}(h)$ - effective number of clusters per sample.

Figure 3 shows the wire, pad and track geometry needed to understand the resolution Equation (3) for the TPC design employing the standard wire/pad design. Figure 4 shows the application of this equation to the PEP-N design, assuming the following parameters: 53 electrons/sample, 19 clusters/sample, drift of 50 cm, single electron diffusion of $450\mu m/\sqrt{\text{cm}}$, wire pitch of 0.4 mm, pad length of 3 cm, pad width of 0.5 cm and magnetic field of 0.32 T. One can see that resolution blows up at large $\Theta$ and $\alpha$ angles as is typical in the standard TPC designs. Table 3 summarizes the expected number of electrons and clusters in various gases, which is useful if one would want to consider the He-based gases. If one would use a conventional fast gas, it is possible to choose a smaller pad size. The 3 cm pad length is probably necessary for the He-based gases.

So far, we assumed the detector based on a standard TPC readout based on the wires and pads such as STAR TPC [6]. However, recently new technologies emerged. For example, if

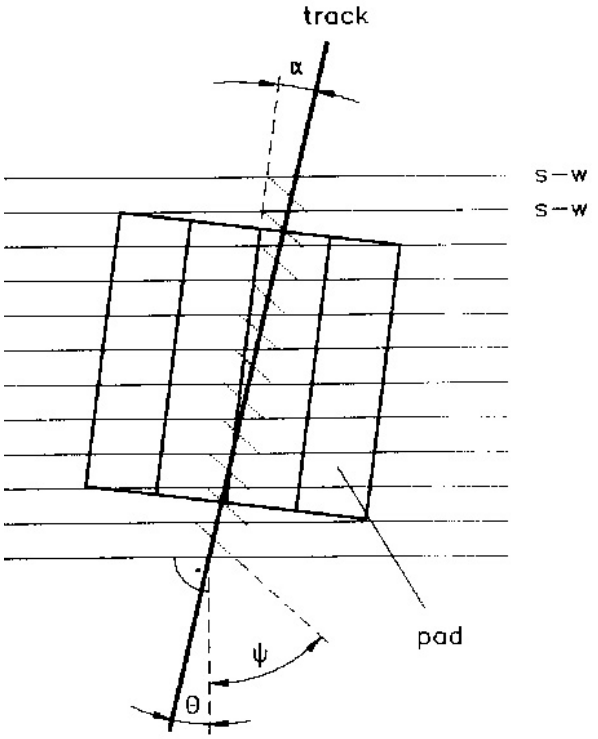


Figure 3: Track, pads and wires and angles needed to understand the resolution calculation.

one would use a wireless design based on the GEM concept, the second term in the resolution equation would not contribute at all.

### 2.4. Triple-GEM Detector with Pads

In view of the resolution argument presented in the previous section, it is tempting to propose the detection design with no wires. On could consider, for example, a detector based on three GEMs in tandem with a pad readout shown in Figure 5. The GEM concept was pioneered by F. Sauli [7] and is being used in the COMPASS experiment [8]. Sauli's group has demonstrated rate capabilities up to 10 MHz/cm$^2$, time resolution of 10 ns (rms) and radiation hardness up to 5C/cm$^2$. The author has also tested the quadruple-GEM with pad readout successfully for the single electron detection [9]. One should also mention that the LHC-b experiment [10] has a strong R&D investigating the triple-GEM with pad readout concept.

In the following, we summarize the advantages and disadvantages of the GEM detection concept:

1. Advantages:
   - No wires.
   - No second term in the resolution equation.
   - More simple construction.
   - Less positive ions into the drift volume.

(a)

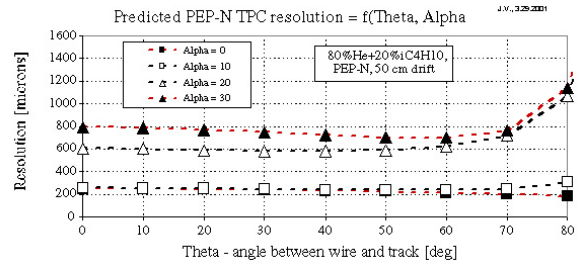


(b)

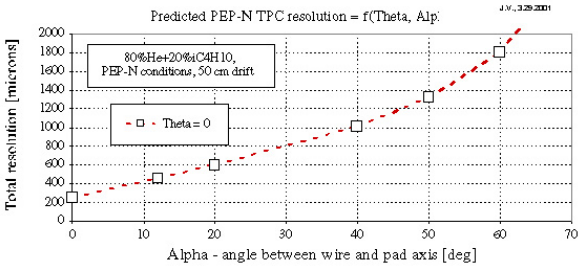


Figure 4: Predicted resolution per sample in the PEP-N TPC in a slow 80%He + 20%$C_4H_{10}$ gas a function (a) $\Theta$ and (b) $\alpha$ angles, defined in Figure 3.

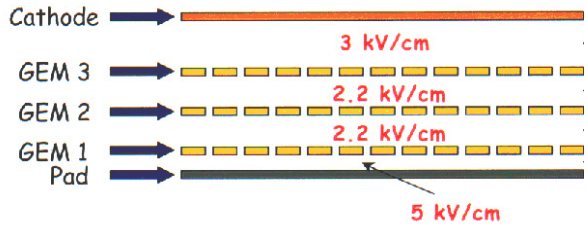


(b)

Figure 5: Triple-GEM with pad readout as tested by the HLHC-b R&D effort.

2. Disadvantages:

   - GEM foil can be permanently damaged.
   - The gain uniformity could be worse.

To guard against damages, one would want to run at as small gas gain as possible, i.e., less than $2-3\times10^3$. As an example, PEP-N would have $\sim 3\times53$ electrons per 3 cm-long sample in 80%He + 20%i$C_4H_{10}$ gas. With gas gain of $2\times10^3$, it will have $\sim 3\times10^5$ electrons available to the amplifier input, which should be possible to obtain a good measurement provided that the electronics noise is kept near $\sigma_{\rm noise}\sim$ 1000el. In PEP-N TPC, one can use longer shaping times (200–250ns).

The gating would be necessary only if the backgrounds would be very large.

One could choose the COMPASS experiment size GEM foil, which would fit well the field cage design proposed in the next chapter.

### 2.5. Field Cage Design

The field cage design is extremely critical for the successful operation of the PEP-N TPC, especially, if one decides to use the slow gases. After considering several possible design choices, I would propose to follow ideas from the ALICE TPC design, which is the most recent TPC application. The main reason is that it provides a very low mass for low energy particles, which is very important for the PEP-N experiment, and also it provides a convenient way to introduce multiple laser beams for the calibration purposes.

The proposed field cage design is shown in Figures 6 and Figure 7. The aluminized Mylar strips are wound around four ceramic rods. With a single layer of these strips, the expected electric field distortions are expected to be less than $10^{-4}$ about 2 cm away from the strips in the ALICE design [11]. The TPC high voltage central plane made of solid Nomex carbon fiber structure, the effect of the grounded beam pipe is de-coupled with field cage structure made of solid self-supporting carbon strips. The laser beams are distributed into the TPC volume by reflections from many mirrors placed in the ceramic rods. The outer field cage is surrounded with a grounded cage made of Hexel panels, which also served as gas envelope. Figure 7 shows the top view and indicates the modular structure of the GEM detectors. The size is chosen to be that same as the COMPASS experiment [8] to simplify the production. The individual modules are identical to allow easy maintenance.

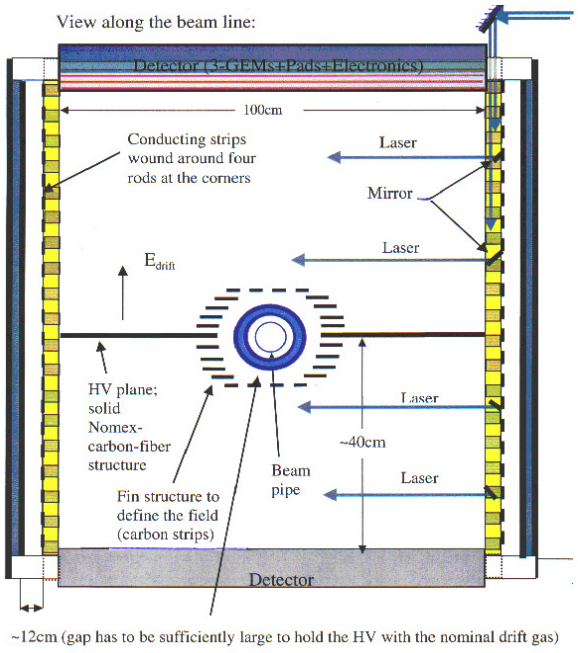


(b)

Figure 6: Field cage–a view along the beam pipe. The field cage is assumed to be built as one unit around the trapped section of the beam pipe to minimize the systematic misalignments. The central HV plane is solid Nomex carbon fiber structure. There are two identical detector sections, each containing nine segments of the triple-GEM detectors with pad readout.

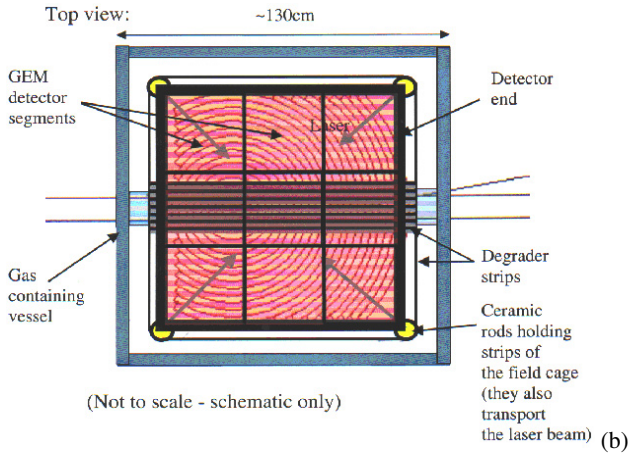


Figure 7: Field cage–top view. The picture also shows the radial pattern of the GEM readout strips ($\sim$ 3 cm long, $\sim$ 5 cm wide), carbon strips along the beam line, field cage with ceramic rods and Mylar strips, and outer Hexel gas containing enclosure.

## 3. CONCLUSION

- Presented design seems to be practical.
- The detector is using a novel triple-GEM structure with the pad readout, which would eliminate the wire-induced $E \times B$ resolution degradation in the detecting plane. It is proposed to use the COMPASS experiment [8] size GEM foils, which would mean $2 \times 9 \times 3$ of such foils per entire PEP-N TPC readout.
- The maximum predicted distortions are less than 1 cm for the fast gases using the DV.06b field map, and less than a few mm for the slow gases. This means that the fast gases are the option if necessary.
- The expected resolution is about 300$\mu$m per single point in track.
- The typical track has 15 points, each sampled with a pad length of 3 cm, which should allow to use the He-based gases.
- The field cage design follows the ALICE design which provides a low mass and easy entry of the laser calibration beams into the TPC volume.
- The capability of a TPC concept to handle a very large number particle densities was clearly demonstrated by the STAR [5] and NA-49 [12] TPC detectors. This is because of a very low gas gain operation reducing the avalanche saturation effects and the ion field distortions to minimum.

## ACKNOWLEGEMENTS

I would like to thank M. Posocco, M. Negrini, G. Bencivenni, R. Baldini, H. Wieman, and T, Mayer for help and useful comments.

## REFERENCES

[1] Langevin, unpublished.
[2] S, Biagi, “Bagbolts-MONTE” computer program.
[3] NA-45-Private communication
[4] G. Rai, A. Arthur, F. Bieser, C.W. Harden, R. Jones, S. Kleinfelder, K. Lee, H.S. Matis, M. Nakamura, C. McParland, D. Nesbitt, G. Odyniec,D. Olson, H.G. Pugh, H.G. Ritter, T.J.M.Symons, H. Wieman, M. Wright and A. Rudge, IEEE Trans. Nucl. Sci. 37, (1990) 56; LBL-28141
[5] Bloom, Ronaldi, “Particle Detection with Drift Chambers,” Springer-Verlag, Berlin, 1994.
[6] STAR experiment, RHIC, Brookhaven Natl. Lab.
[7] F. Sauli, Nucl. Instr. & Meth., A386 (1997) 531.
[8] Compass experiment, CERN.
[9] J. Va’vra and A. Sharma, SLAC-PUB-8785, March 6, 2001, also presented at Vienna Conference, February 2001.
[10] G. Benciveni, LHC-b, private communication, paper related to the LHC-b R&D effort also presented at Vienna Conference, February 2001.
[11] T. Mayer, ALICE experiment, private communication.
[12] NA-49 experiment, CERN.

Table I Summary of distortion calculations by the author in the PEP-N TPC for electron drift of 50 cm at radial distance of 50 cm.

a) Distortions = f(gas choice):

| Gas | Field map | E-drift [V/cm] | dx [cm] | dy [cm] |
|---|---|---|---|---|
| $80\%Ar + 20\%CH_4$ | DV.02 | 400 | $-4.2$ | $-4.9$ |
| $80\%He + 20\%CO_2$ | DV.02 | 400 | $-.07$ | $-0.9$ |
| $80\%He + 19\%CO_2 + 1\%CH_4$ | DV.02 | 400 | $-0.1$ | $-0.91$ |
| $80\%He + 15\%CO_2 + 5\%CH_4$ | DV.02 | 400 | $-0.12$ | $-1.03$ |
| $80\%He + 15\%CO_2 + 5\%iC_4H_{10}$ | DV.02 | 400 | $-0.1$ | $-1.0$ |
| $80\%He + 20\%iC_4H_{10}$ | DV.02 | 400 | $-0.3$ | $-1.5$ |

b) Distortions = f(TPC drift field):

| Gas | Field map | E-drift [V/cm] | dx [cm] | dy [cm] |
|---|---|---|---|---|
| $80\%Ar + 20\%CH_4$ | DV.02 | 400 | $-4.2$ | $-4.9$ |
| $80\%Ar + 20\%CH_4$ | DV.02 | 200 | $-6.8$ | $-4.2$ |
| $80\%He + 20\%CO_2$ | DV.02 | 400 | $-.07$ | $-0.9$ |
| $80\%He + 20\%CO_2$ | DV.02 | 200 | $-0.1$ | $-0.9$ |

c) Distortions = f(field map):

| Gas | Field map | E-drift [V/cm] | dx [cm] | dy [cm] |
|---|---|---|---|---|
| $80\%Ar + 20\%CH_4$ | DV.02 | 400 | $-4.2$ | $-4.9$ |
| $80\%Ar + 20\%CH_4$ | DV.03 | 400 | $-2.7$ | $-2.9$ |
| $80\%He + 20\%CO_2$ | DV.02 | 400 | $-.07$ | $-0.9$ |
| $80\%He + 20\%CO_2$ | DV.03 | 400 | $-.04$ | $-0.5$ |
| $80\%Ar + 20\%CH_4$ | DV.06b | 400 | $-1.0$ | $-1.04$ |
| $80\%He + 20\%CO_2$ | DV.06b | 400 | $-.08$ | $-0.25$ |

Table II Typical maximum distortion in various TPC designs and a final reduction factor achieved to get a final required resolution.

| TPC | Maximum distortion [cm] | A final reduction factor achieved |
|---|---|---|
| CRID | $\sim 1$ | $\sim 10$ |
| STAR | $\sim 0.2 - 0.3$ | $\sim 5$ |
| NA-45 | $\sim 11$ | $\sim 600$ within a factor of 2 of achieving this) |
| PEP-N | $\sim 1$ fast gave, DV.06b) | $\sim 50$ (planned) |
| PEP-N | $\sim 0.2$ (slow gas, DV.06b) | $\sim 10$ (planned) |

Table III Typical expected number of electron and clusters in various gas candidates for the PEP-N TPC.

| Gas | No. of electrons per 3 cm sample | No. of clusters per 3 cm sample |
|---|---|---|
| $80\%Ar + 20\%CH_4$ | $\sim$267 | $\sim$74 |
| $80\%He + 20\%CO_2$ | $\sim$78 | $\sim$28 |
| $80\%He + 19\%CO_2 + 1\%CH_4$ | $\sim$77 | $\sim$28 |
| $80\%He + 15\%CO_2 + 5\%CH_4$ | $\sim$72 | $\sim$27 |
| $80\%He + 15\%CO_2 + 5\%iC_4H_{10}$ | $\sim$98 | $\sim$36 |
| $80\%He + 20\%C_4H_{10}$ | $\sim$158 | $\sim$58 |